



HAL
open science

The atmospheric chemistry of sulphuryl fluoride, SO₂F₂

T. J. Dillon, A. Horowitz, J. N. Crowley

► **To cite this version:**

T. J. Dillon, A. Horowitz, J. N. Crowley. The atmospheric chemistry of sulphuryl fluoride, SO₂F₂. Atmospheric Chemistry and Physics Discussions, 2007, 7 (5), pp.15213-15249. <hal-00303152>

HAL Id: hal-00303152

<https://hal.science/hal-00303152v1>

Submitted on 18 Jun 2008

HAL is a multi-disciplinary open access archive for the deposit and dissemination of scientific research documents, whether they are published or not. The documents may come from teaching and research institutions in France or abroad, or from public or private research centers.

L'archive ouverte pluridisciplinaire HAL, est destinée au dépôt et à la diffusion de documents scientifiques de niveau recherche, publiés ou non, émanant des établissements d'enseignement et de recherche français ou étrangers, des laboratoires publics ou privés.



HAL Authorization

**Atmospheric
chemistry of SO₂F₂**

T. J. Dillon et al.

The atmospheric chemistry of sulphuryl fluoride, SO₂F₂

T. J. Dillon, A. Horowitz, and J. N. Crowley

Max Planck Institute for Chemistry, Mainz, Germany

Received: 4 October 2007 – Accepted: 12 October 2007 – Published: 25 October 2007

Correspondence to: T. J. Dillon (dillon@mpch-mainz.mpg.de)

Title Page

Abstract

Introduction

Conclusions

References

Tables

Figures

◀

▶

◀

▶

Back

Close

Full Screen / Esc

Printer-friendly Version

Interactive Discussion

EGU

Abstract

The atmospheric chemistry of sulphuryl fluoride, SO_2F_2 , was investigated in a series of laboratory studies. A competitive rate method, using pulsed laser photolysis (PLP) to generate $\text{O}(^1\text{D})$ coupled to detection of OH by laser induced fluorescence (LIF), was used to determine the overall rate coefficient for the reaction $\text{O}(^1\text{D}) + \text{SO}_2\text{F}_2 \rightarrow$ products (R1) of k_1 (220–300 K) $= (1.3 \pm 0.2) \times 10^{-10} \text{ cm}^3 \text{ molecule}^{-1} \text{ s}^{-1}$. Monitoring the $\text{O}(^3\text{P})$ product (R1a) enabled the contribution (α) of the physical quenching process (in which SO_2F_2 is not consumed) to be determined as α_1 (225–296 K) $= (0.55 \pm 0.04)$. Separate, relative rate measurements at 298 K provided a rate coefficient for reactive loss of $\text{O}(^1\text{D})$, k_{1b} , of $(5.8 \pm 0.8) \times 10^{-11} \text{ cm}^3 \text{ molecule}^{-1} \text{ s}^{-1}$ in good agreement with the value calculated from $(1 - \alpha) \times k_1 = (5.9 \pm 1.0) \times 10^{-11} \text{ cm}^3 \text{ molecule}^{-1} \text{ s}^{-1}$. Upper limits for the rate coefficients for reaction of SO_2F_2 with OH (R2, using PLP-LIF), and with O_3 (R3, static reactor) were determined as k_2 (294 K) $< 1 \times 10^{-15} \text{ cm}^3 \text{ molecule}^{-1} \text{ s}^{-1}$ and k_3 (294 K) $< 1 \times 10^{-23} \text{ cm}^3 \text{ molecule}^{-1} \text{ s}^{-1}$. In experiments using the wetted-wall flow tube technique, no loss of SO_2F_2 onto aqueous surfaces was observed, allowing an upper limit for the uptake coefficient of γ (pH 2–12) $< 1 \times 10^{-7}$ to be determined. These results indicate that SO_2F_2 has no significant loss processes in the troposphere, and a very long stratospheric lifetime. Integrated band intensities for SO_2F_2 infrared absorption features between 6 and 19 μm were obtained, and indicate a significant global warming potential for this molecule. In the course of this work, ambient temperature rate coefficients for the reactions $\text{O}(^1\text{D})$ with several important atmospheric species were determined. The results (in units of $10^{-10} \text{ cm}^3 \text{ molecule}^{-1} \text{ s}^{-1}$), $k_{(\text{O}^1\text{D}+\text{N}_2)} = (0.33 \pm 0.06)$; $k_{(\text{O}^1\text{D}+\text{N}_2\text{O})} = (1.47 \pm 0.2)$ and $k_{(\text{O}^1\text{D}+\text{H}_2\text{O})} = (1.94 \pm 0.5)$ were in good agreement with other recent determinations.

Title Page

Abstract

Introduction

Conclusions

References

Tables

Figures

◀

▶

◀

▶

Back

Close

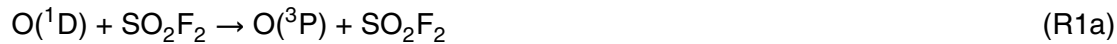
Full Screen / Esc

Printer-friendly Version

Interactive Discussion

1 Introduction

Sulphuryl fluoride, SO₂F₂, (Vikane™, Zythor™, ProFume™) is a widely used fumigant of timber, buildings, construction materials and vehicles. 30 years have passed since SO₂F₂ was first mentioned in the context of a potential influence on stratospheric sulphur chemistry (Crutzen, 1976) and in this period the use of SO₂F₂ has been extended to the food processing and agriculture industries as a replacement for CH₃Br (banned under the Montreal protocol). The main consumer of SO₂F₂ is the U.S. state of California where annual usage has exceeded 10⁶ Kg since 1999 (Kollman, 2006). Indeed, SO₂F₂ has recently been detected for the first time in ambient air samples (Mühle et al., 2006). These first ambient measurements of SO₂F₂ provided the motivation for us to undertake a series of laboratory investigations into the kinetics of reactions of SO₂F₂, with atmospheric oxidants/surfaces for which no data existed. The UV absorption spectrum of SO₂F₂ has been measured (Pradayrol et al., 1996) and the results demonstrate that photolysis is an insignificant loss process in the troposphere. Cady and Misra (1974) have measured hydrolysis rates for SO₂F₂ in aqueous solutions. Their results indicate that hydrolysis is slow in acidic or neutral conditions, but may be an efficient atmospheric loss process in basic conditions (i.e. at the ocean surface). There are no published data regarding potential gas-phase atmospheric loss processes for SO₂F₂, or heterogeneous uptake to surfaces. Nonetheless, an upper-limit to the atmospheric lifetime of SO₂F₂ of τ ≲ 4.5 years has been suggested (European Union Report, 2005). In the present study, a variety of laboratory techniques were used to measure rate coefficients, *k*, for the gas-phase Reactions (R1–R3) of SO₂F₂ with the atmospheric oxidants O(¹D), OH, and O₃, and the rate of heterogeneous uptake of SO₂F₂ to aqueous surfaces (Reaction R4):



Title Page

Abstract

Introduction

Conclusions

References

Tables

Figures

◀

▶

◀

▶

Back

Close

Full Screen / Esc

Printer-friendly Version

Interactive Discussion



Note that SO_2F_2 is consumed in all processes except for Reaction (R1a). The kinetic data obtained in this work is used to estimate the lifetime of SO_2F_2 in the atmosphere and thus its impact on various aspects of atmospheric science.

2 Experimental

5 The experiments were conducted using a variety of laboratory techniques and equipment. The gas phase experiments utilised both real time techniques (pulsed laser photolysis coupled to laser induced fluorescence (PLP-LIF) or resonance fluorescence (PLP-RF)), a relative rate technique with Fourier transform infrared spectroscopy (RR-FTIR) and a simple static mixing approach with UV analysis. A potential heterogeneous
10 loss process (uptake of SO_2F_2 to aqueous surfaces) was investigated using the wetted-wall flow tube technique (WWFT). These are described in turn below.

2.1 PLP-LIF/RF

The PLP-LIF and PLP-RF techniques have been used in this laboratory to study reactions of $\text{O}(^1\text{D})$ (Dillon et al., 2007), $\text{O}(^3\text{P})$ (Teruel et al., 2004), IO (Dillon et al., 2006)
15 and OH (Wollenhaupt et al., 2000; Karunanandan et al., 2007). The experimental set-up has been described in detail previously (see for example Wollenhaupt et al. (2000), which includes a schematic diagram of the apparatus) and is outlined only briefly here. Experiments were conducted in a 500 cm^3 quartz reactor, the temperature of which was regulated by circulating a cryogenic fluid through the outer jacket, and monitored
20 with a J-Type thermocouple. The reactor pressure was monitored with a capacitance

Title Page

Abstract

Introduction

Conclusions

References

Tables

Figures

◀

▶

◀

▶

Back

Close

Full Screen / Esc

Printer-friendly Version

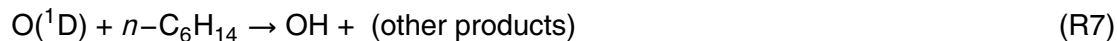
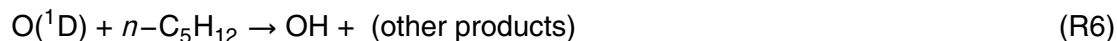
Interactive Discussion

manometer. Gas flow rates of 300–2500 cm³ (STP) min⁻¹ ensured that a fresh gas sample was available for photolysis at each laser pulse. Chemistry was initiated by an excimer laser (Lambda Physik) operating at 248 nm (KrF).

Fluorescence from OH was detected by a photomultiplier tube (PMT) shielded by 309 nm (interference) and BG 26 (glass cut-off) filters. Excitation of the A²Σ (ν=1)←X²Π (ν=0), Q₁₁ (Eq. 1) transition of OH at 281.997 nm was achieved using the frequency doubled emission from a Nd-YAG (Quantel) pumped dye laser (Lambda Physik/rhodamine 6G).

Resonance emission used to detect O(³P) at ~131 nm was generated by microwave discharge (80 W) through 99.996% He at ~3 Torr, and passed through a set of baffles and a CaF₂ window (to remove radiation from excited H or N atoms) before entering the cell perpendicular to both the pulsed emission from the excimer photolysis laser and the VUV photomultiplier detection axis. Fluorescence was gathered by a *f*=1.4 telescopic arrangement and focussed onto the active area of the VUV photomultiplier. Time dependent O(³P) signals were amplified, digitised and counted by a multichannel scaler usually operating at a resolution of 5 μs per channel, and averaging 1000 decay profiles.

In the experiments designed to study Reaction (R1), O(¹D) was generated by the 248 nm photolysis of O₃ (Reaction R5). O(¹D) was not detected directly, but converted to OH by reaction with a straight-chain alkane *n*-C₅H₁₂ (Reaction R6) or *n*-C₆H₁₄ (Reaction R7), and in a few experiments H₂O (Reaction R8).


[Title Page](#)
[Abstract](#)
[Introduction](#)
[Conclusions](#)
[References](#)
[Tables](#)
[Figures](#)
[◀](#)
[▶](#)
[◀](#)
[▶](#)
[Back](#)
[Close](#)
[Full Screen / Esc](#)
[Printer-friendly Version](#)
[Interactive Discussion](#)

The 248 nm photolysis of H_2O_2 (Reaction R9) was used to generate OH in the experiments to determine k_2 (294 K).



Typically, laser fluences of 12 mJ cm^{-2} per pulse were used to generate $[\text{O}(^1\text{D})]$ or $[\text{OH}]$ of $\approx 2 \times 10^{11} \text{ molecule cm}^{-3}$. Concentrations of the radical precursors O_3 ($< 2 \times 10^{12} \text{ molecule cm}^{-3}$) and H_2O_2 ($\sim 3 \times 10^{13} \text{ molecule cm}^{-3}$) were determined optically by monitoring the attenuation of light (185 or 254 nm) from a Hg lamp transmitting a 43.8 cm absorption cell situated downstream of the reactor. Due to the small absorption cross-sections of SO_2F_2 at suitable wavelengths, optical measurements of $[\text{SO}_2\text{F}_2]$ were not possible. Concentrations of the excess reagents SO_2F_2 , $n\text{-C}_5\text{H}_{12}$, $n\text{-C}_6\text{H}_{14}$, N_2 , N_2O , and H_2O were therefore determined by manometric methods to an estimated (minimum) accuracy of $\pm 15\%$ ($\pm 30\%$ for H_2O) based upon uncertainties in (calibrated) mass flow rates, T and P .

2.2 RR-FTIR

Relative rate experiments were carried out in a cylindrical quartz reactor cell of volume 45 l, fitted with internal multipass optics to give an effective optical path-length of 28 m (Raber and Moortgat, 2000). Photolysis was provided by 9 UV lamps (Philips, TUV 40 W) evenly distributed around the outside of the reactor and flushed with compressed air to prevent warming of the ambient air directly in contact with the reactor surface. Static mixtures of O_3 , SO_2F_2 (or SF_6) and N_2O were prepared in the cell and approximate concentrations determined manometrically. The relative rate experiments were conducted at a total pressure of ≈ 200 Torr (He) and the gas mixture was left to stand for > 20 min to ensure mixing and thermalization. FTIR spectra ($450\text{--}2000 \text{ cm}^{-1}$, 0.5 cm^{-1} resolution, typically 256 co-added scans) were recorded prior to, and at regular intervals after UV irradiation using a Bomem DA-008 spectrometer with a MCT detector. The variation of the concentration of N_2O and SO_2F_2 with irradiation time was determined by repeating the alternating irradiation and spectra acquisition steps, and

[Title Page](#)[Abstract](#)[Introduction](#)[Conclusions](#)[References](#)[Tables](#)[Figures](#)[◀](#)[▶](#)[◀](#)[▶](#)[Back](#)[Close](#)[Full Screen / Esc](#)[Printer-friendly Version](#)[Interactive Discussion](#)

by preparing new mixtures which were then photolysed for different exposure times. The exposure times were always shorter than 300 s and no change in the cell temperature was observed over this period. The relative change in the concentration of the two reactants was derived by fitting the observed spectra to the initial reference using absorption features between 578 and 603 cm^{-1} for N_2O and between 1438 and 1566 cm^{-1} for SO_2F_2 .

The same spectrometer was used to measure quantitative IR spectrum of SO_2F_2 , but using a 50 cm^3 volume, single pass glass optical absorption cell (optical path-length 15 cm) equipped with Si optical windows.

2.3 WWFT

The uptake of SO_2F_2 to aqueous surfaces was investigated using the wetted-wall flow tube technique. The apparatus used has been described in previous publications (Fickert et al., 1998, 1999) and only salient features are given here. SO_2F_2 was introduced via a movable injector into a laminar flow tube reactor (internal radius = 7.75 mm) operated at a pressure of about 250–290 Torr and at $T=277\text{ K}$. The bulk gas was He, flowed at $\approx 300\text{ sccm}$, resulting in a Reynolds number of 2.5, and a linear velocity of $\approx 4\text{ cm s}^{-1}$. Flow rates were monitored by freshly calibrated mass flow controllers and are expected to be accurate to a few percent. The pressure was monitored with a 1000 Torr capacitance manometer. The inner wall of the flow tube was coated with a slowly flowing aqueous film which was prepared from bulk solutions with pH adjusted to 2, 4.5 or 12. The thickness and speed of the liquid film were calculated as described previously (Fickert et al., 1998) to be $\approx 100\ \mu\text{m}$ and $3\text{--}4\text{ cm s}^{-1}$, respectively.

The contact time between SO_2F_2 and the aqueous film was varied by translating the moveable injector using a computer controlled linear drive to accurately maintain axial alignment between the injector and the aqueous film. Using the relatively slow gas flows indicated above, contact times of up to about 8 s were achieved. SO_2F_2 exiting the flow tube at a concentration of approximately $5 \times 10^{13}\text{ molecule cm}^{-3}$ was detected

Title Page

Abstract

Introduction

Conclusions

References

Tables

Figures

◀

▶

◀

▶

Back

Close

Full Screen / Esc

Printer-friendly Version

Interactive Discussion

by electron bombardment positive ion mass spectrometry (MS) at $m/z=83$. This was the strongest ion signal when the MS was operated with an electron energy of 70 eV.

2.4 Chemicals

He (Westfalen, 99.999%), N₂ (Messer 99.999), O₂ (Messer, 99.998), Synthetic Air (Messer, 20.5 % O₂ in N₂), N₂O (Messer, 99.5%), SO₂F₂(ABCR, 99%) and SF₆ (Messer 1.99% in He 99.9%) were used without further purification. O₃ was prepared using a commercial ozoniser (Ozomat), trapped on silica gel at $T=195$ K, and flushed with He to remove O₂ before dilution ($\sim 10^{-4}$) in He and storage in blackened glass bulbs. *n*-C₅H₁₂ (Aldrich “wasserfrei” 99+ %) and *n*-C₆H₁₄ (neoLab >95%) were subject to repeated freeze-pump-thaw cycles at 77 K prior to dilution and storage. Aqueous solutions for the WWFT experiments were prepared using “milli-Q” de-ionised water, with the pH adjusted by addition of H₂SO₄ or NaOH.

3 Results

The determination of kinetic parameters for Reactions (R1–R4) are detailed in Sects. 3.1–3.3 below. As this was the first comprehensive study of the atmospheric chemistry of SO₂F₂, comparison with literature data was rarely possible. Where possible however, the experimental methods used here were validated by the concurrent study of well-characterised processes, such as the reactions of O(¹D) with the important atmospheric species N₂, N₂O, H₂O and SF₆. The infrared absorption spectrum of SO₂F₂ is described in Sect. 3.4 and the uptake of SO₂F₂ to aqueous solutions in Sect. 3.5. The atmospheric implications of the results obtained are discussed in Sect. 3.6.

Title Page

Abstract

Introduction

Conclusions

References

Tables

Figures

◀

▶

◀

▶

Back

Close

Full Screen / Esc

Printer-friendly Version

Interactive Discussion

3.1 Kinetics and products of $O(^1D)+SO_2F_2 \rightarrow$ products (Reaction R1)

3.1.1 Determination of overall rate coefficients k_1 (220–300 K) for Reaction (R1)

Absolute values for $k_1(T)$ were determined by a competitive rate method, similar to that employed by Blitz et al. (2004). This method relies on the fact that the kinetics of product formation are governed by the rate of decay of the precursor species. Specifically in this work, where the LIF detection of OH is used as a spectroscopic marker for $O(^1D)$:

$$\frac{d[O(^1D)]}{dt} = \frac{-d[OH]}{dt} \quad (1)$$

PLP generation (Reaction R5) of $O(^1D)$ in the presence of $n-C_6H_{14}$ facilitated rapid conversion (Reaction R7) of $O(^1D)$ to OH. Figure 1 displays an example of an OH LIF profile recorded at $[O_3] \approx 1 \times 10^{12}$, $[n-C_6H_{14}] = 2.1 \times 10^{13}$ molecule cm^{-3} and $P = 42$ Torr (1 Torr = 1.333 mBar) of He (bath gas) at $T = 298$ K. The open circles in Fig. 1 show an OH LIF profile, recorded upon addition of $[SO_2F_2] = 2.3 \times 10^{14}$ molecule cm^{-3} to the reaction mixture. The introduction of SO_2F_2 results in the observation of a smaller OH signal, which is formed on a shorter timescale as SO_2F_2 competes to destroy $O(^1D)$. Pseudo first-order conditions of both $[n-C_6H_{14}]$ and $[SO_2F_2] \gg [O(^1D)]$ and $[OH]$ applied, and the data were therefore analysed with the appropriate kinetic expression (Eq. 2):

$$[OH]_t = A \times \{\exp(-Bt) - \exp(-Ct)\} \quad (2)$$

where A is proportional to the initial $[O(^1D)]$, B is the approximate pseudo first-order rate coefficient for OH loss (dominated by slow transport out of the LIF volume), and the parameter of interest C is the 1st-order rate coefficient for OH formation (equivalent to $O(^1D)$ loss, see Eq. (1) above).

$$C = k_1[SO_2F_2] + k_7[n-C_6H_{14}] + k_{\text{loss-}O(^1D)} \quad (3)$$

The parameter $k_{\text{loss-}O(^1D)}$ accounts for reaction of $O(^1D)$ with O_3 , bath-gas (He) and trace impurities therein. Experimentally determined values of C were obtained with a

[Title Page](#)[Abstract](#)[Introduction](#)[Conclusions](#)[References](#)[Tables](#)[Figures](#)[◀](#)[▶](#)[◀](#)[▶](#)[Back](#)[Close](#)[Full Screen / Esc](#)[Printer-friendly Version](#)[Interactive Discussion](#)

Title Page

Abstract

Introduction

Conclusions

References

Tables

Figures

◀

▶

◀

▶

Back

Close

Full Screen / Esc

Printer-friendly Version

Interactive Discussion

fixed n -C₆H₁₄ concentration and various values of [SO₂F₂] so that that a plot of C versus associated [SO₂F₂] (Fig. 2, solid squares) has a gradient equivalent to k_1 (298 K), and an intercept of $k_7[n\text{-C}_6\text{H}_{14}] + k_{\text{loss-O}(^1\text{D})}$ (Eq. 3). An un-weighted linear fit to the dataset displayed (solid line) yields k_1 (298 K) = $(1.39 \pm 0.1) \times 10^{-10} \text{ cm}^3 \text{ molecule}^{-1} \text{ s}^{-1}$. Experiments were repeated over the range of $218 < T/\text{K} < 300$, using both n -C₅H₁₂ and n -C₆H₁₄ to convert O(¹D) to OH. Statistically similar values of $k_1(T)$ were obtained (Table 1).

The kinetic analysis was validated in 3 ways. First, in the presence of SO₂F₂, OH profiles were recorded in which the photolysis laser energy was varied by a factor of 5. No systematic change in C was observed, indicating that secondary chemistry did not perturb the OH kinetics. Second, rate coefficients for the reactions of O(¹D) with n -C₅H₁₂ (Reaction R6) and n -C₆H₁₄ (Reaction R7) were determined by recording OH profiles at different alkane concentrations in the absence of SO₂F₂. The plots of parameter C (obtained from fitting expression (2) to the data) versus [n -C₅H₁₂] or [n -C₆H₁₄] yielded k_6 (298 K) = $(5.4 \pm 0.4) \times 10^{-10} \text{ cm}^3 \text{ molecule}^{-1} \text{ s}^{-1}$ and k_7 (298 K) = $(5.8 \pm 0.5) \times 10^{-10} \text{ cm}^3 \text{ molecule}^{-1} \text{ s}^{-1}$, in excellent agreement with the only previous absolute determinations (Dillon et al., 2007) and an evaluation of earlier relative rate determinations (Schofield, 1978). Third, the competitive rate method was employed to determine rate coefficients for the well-characterised Reactions (R10) and (R11):



The procedure was identical to that described above, and many experiments were carried out back-to-back with the determinations of k_1 . The results, listed in Table 1 and illustrated in Fig. 2 for N₂O, are k_{10} (298 K) = $(0.33 \pm 0.06) \times 10^{-10} \text{ cm}^3 \text{ molecule}^{-1} \text{ s}^{-1}$ and k_{11} (298 K) = $(1.45 \pm 0.2) \times 10^{-10} \text{ cm}^3 \text{ molecule}^{-1} \text{ s}^{-1}$, which are in good agreement with the evaluated literature (Sander et al., 2006; Atkinson et al., 2007) and other recent

determinations (Blitz et al., 2004; Dunlea and Ravishankara, 2004b; Strekowski et al., 2004; Carl, 2005; Takahashi et al., 2005). The good agreement indicates that potential problems associated with formation of vibrationally excited OH radicals are insignificant and give confidence in the values of k_1 obtained in this work.

In some additional experiments, H_2O was used to convert $\text{O}(^1\text{D})$ to OH (Reaction R8). The procedures detailed above were used to obtain k_8 directly, and k_{10} ($\text{O}(^1\text{D})+\text{N}_2$). The results are in satisfactory agreement with the literature. Some experiments were also conducted with a $\text{O}(^1\text{D})/\text{H}_2\text{O}/\text{SO}_2\text{F}_2$ reaction system with the aim of a further, independent measurement of k_1 . However, the LIF profiles generated in the presence of SO_2F_2 were characterised by the expected rapid OH formation due to $\text{O}(^1\text{D})$ loss in Reactions (R1) and (R8), followed by a secondary slow OH formation process. The slow OH source was not evident in back-to-back experiments where SO_2F_2 was absent or replaced by N_2 . A possible explanation for these observations is that a product of Reaction (R1), not produced in Reactions (R8) or (R10) may itself be an OH precursor. It appears likely that F-atoms, formed as a product of SO_2F_2 destruction (R1b) by $\text{O}(^1\text{D})$, are converted by H_2O to OH in the well-characterised Reaction (R12):



Numerical simulation of these experiments using the evaluated literature value k_{12} (298 K) = $1.4 \times 10^{-11} \text{ cm}^3 \text{ molecule}^{-1} \text{ s}^{-1}$ demonstrated that Reaction (R12) could indeed account for the secondary OH observed in the presence of SO_2F_2 if a yield of $\approx 20\%$ F-atoms from Reaction (R1) was assumed. This result, implying that SO_2F_2 is destroyed in Reaction (R1), is only semi-quantitative, and prompted experiments (see Sects. 3.1.2 and 3.1.3) to quantify the relative importance of reaction channels (R1a) and (R1b).

Although there are no experimental data with which to compare our value for k_1 , we note that the result is consistent with the predicted value of $(1.1 \pm 0.8) \times 10^{-10} \text{ cm}^3 \text{ molecule}^{-1} \text{ s}^{-1}$ based on an ionisation potential/collision cross

[Title Page](#)[Abstract](#)[Introduction](#)[Conclusions](#)[References](#)[Tables](#)[Figures](#)[◀](#)[▶](#)[◀](#)[▶](#)[Back](#)[Close](#)[Full Screen / Esc](#)[Printer-friendly Version](#)[Interactive Discussion](#)

section relationship presented by Dillon et al. (2007).

3.1.2 Physical quenching (Reaction R1a) – the yield of O(³P) from Reaction (R1)

Figure 3 displays an example of an O(³P) RF profile (RF_{SO₂F₂}) obtained following photolysis of O₃ (Reaction R5) in the presence of [SO₂F₂]=1.4×10¹⁴ molecule cm⁻³ at *P*=42 Torr and *T*=296 K. The yield (*k*_{1*a*}/*k*₁) of O(³P) from Reaction (R1) was determined by using the reaction of O(¹D) with N₂ (R10), for which the unity yield of O(³P) is well established, to calibrate the data. The SO₂F₂ was replaced by a kinetically matched amount of N₂ (*k*₁ [SO₂F₂]=*k*₁₀[N₂]) and the RF signal (see Fig. 3 open circles) from Reaction (R10), RF_{N₂} was then recorded. RF signals (RF₀) were also obtained in the absence of SO₂F₂ or N₂, to quantify the background level of O(³P) produced directly from O₃ photolysis (Dunlea et al., 2004) and by reactions of O(¹D) with impurities (N₂ or O₂ in the bath gas He). These 3 back-to-back datasets were used to generate RF_{ratio}, the (corrected for background) ratio of RF signals according to expression (2):

$$RF_{\text{ratio}} = \frac{RF_{\text{SO}_2\text{F}_2} - \text{BG}}{RF_{\text{N}_2} - \text{BG}} \quad (4)$$

where

$$\text{BG} = RF_0 \times \frac{k_{\text{loss_O(1D)}}}{k_1[\text{SO}_2\text{F}_2]} = RF_0 \times \frac{k_{\text{loss_O(1D)}}}{k_{10}[\text{N}_2]}$$

Figure 3 shows the resulting time-resolved RF_{ratio}, which is equivalent to the product yield for O(³P) from Reaction (R1): *k*_{1*a*}/*k*₁=(0.56±0.01). The process was repeated for different kinetically matched amounts of SO₂F₂ and N₂, with the corrections for background O(³P) (never more than 20%) smaller for larger [SO₂F₂]. The results are displayed in Table 2, which shows a consistent value of *k*_{1*a*}/*k*₁=(0.55±0.04) at around ambient temperature. Similar results were obtained at *T*=225 K.

RF detection of O(³P) was found to be less suitable for the determination of the absolute rate coefficients, *k*₁(*T*). As is evident from Fig. 3, the data close to *t*=0, where

Title Page

Abstract

Introduction

Conclusions

References

Tables

Figures

◀

▶

◀

▶

Back

Close

Full Screen / Esc

Printer-friendly Version

Interactive Discussion

the fast Reaction (R1) occurs, is not particularly well resolved, and in some experiments was distorted by a strong radio-frequency signal from the excimer laser pulse.

3.1.3 Relative rate determinations of k_{1b}

Mixtures containing SO_2F_2 and N_2O (both at concentrations of $9\text{--}15 \times 10^{14}$ molecule cm^{-3}) and O_3 in He bath gas were photolysed for between 15 and 300 s to result in measurable changes (up to 15%) in the SO_2F_2 and N_2O concentrations. The fractional depletion of both species was limited by the concentration of O_3 , which was completely destroyed, resulting in the disappearance of its 1042 cm^{-1} absorption feature. The initial O_3 concentration (this parameter is not needed in the kinetic analysis) could not be monitored as accessible absorption bands were optically black.

The intense absorption feature of SO_2F_2 centred at 1504 cm^{-1} was generally used for determination of the SO_2F_2 depletion factor after photolysis. The depletion factor was obtained by least-squares fitting of the pre- and post-photolysis spectra in the $1438\text{--}1566 \text{ cm}^{-1}$ range. The relative change in N_2O over the same period was obtained in a similar manner using the single absorption feature around 590 nm. Fitted N_2O and SO_2F_2 spectra, showing the spectral ranges used and the fit-residuals are given in Fig. 4. Use of the stronger N_2O feature at $\approx 1285 \text{ cm}^{-1}$ was not possible due to overlap with a SO_2F_2 absorption band. Owing to the use of several data points the statistical error (2σ) in determination of the relative changes in SO_2 or N_2O concentration was $\approx 6 \times 10^{-4}$ and $\approx 5 \times 10^{-3}$, respectively.

Use of parts (or all of) the triplet feature of SO_2F_2 between 530 and 560 cm^{-1} (see complete IR spectrum presented in Sect. 3.4) gave similar results but with reduced precision.

In the absence of O_3 , neither N_2O nor SO_2F_2 were measurably depleted by photolysis, nor by dark/wall losses. Additional support for the contention that both N_2O and SO_2F_2 were removed only by reaction with $\text{O}(^1\text{D})$ and that mixing/segregation effects

Title Page

Abstract

Introduction

Conclusions

References

Tables

Figures

◀

▶

◀

▶

Back

Close

Full Screen / Esc

Printer-friendly Version

Interactive Discussion

could be ruled out, was obtained by conducting experiments in which SO₂F₂ was replaced by SF₆. In this case, although N₂O was depleted, SF₆, a molecule with very low reactivity to O(¹D) (Sander et al., 2006) was unchanged.

The relative changes in SO₂F₂ and N₂O concentrations were analysed using the standard relation

$$\ln \left(\frac{[\text{SO}_2\text{F}_2]_0}{[\text{SO}_2\text{F}_2]} \right) = \frac{k_1}{k_{11}} \cdot \ln \left(\frac{[\text{N}_2\text{O}]_0}{[\text{N}_2\text{O}]} \right) \quad (5)$$

The complete data set is displayed in Fig. 5, in which the solid line is the least squares fit to the data as described by Eq. (5). The slope of the fit line gives the rate constant ratio $k_1/k_{11}=(0.411\pm 0.012)$. Using a rate coefficient for reaction of N₂O with O(¹D) of 1.4×10^{-10} molecule cm⁻³, from recent work (Dunlea and Ravishankara, 2004a; Carl, 2005; Takahashi et al., 2005) and from this study, k_1/k_{11} can be converted to an absolute rate coefficient; $k_{1b}=(5.8\pm 0.01)\times 10^{-11}$ cm³ molecule⁻¹ s⁻¹. Since in this system no evidence was found for interference from unwanted photolysis and/or dark reactions we estimate that our relative ratio is accurate within ~10% to which we add the error propagated from the reference reaction, also estimated at 10%. Accordingly, the present determination of k_{1b} is $(5.8\pm 0.8)\times 10^{-11}$ cm³ molecule⁻¹ s⁻¹. This result is in good agreement with the value calculated from the results obtained above of overall rate coefficient $k_1=(1.3\pm 0.2)\times 10^{-11}$ cm³ molecule⁻¹ s⁻¹ and product yield of O(³P) $\alpha=0.55\pm 0.04$, whereby $k_{1b}=(1-\alpha)\times k_1=(5.9\pm 1.0)\times 10^{-11}$ cm³ molecule⁻¹ s⁻¹.

The infra-red spectra obtained following photolysis were inspected for formation of IR-active products including NO, SO₂, FNO, FNO₂ and SOF₂, none of which were observed. We have presented evidence (Sect. 3.1.1) that F atoms are formed in the reaction of O(¹D) with SO₂F₂. The fate of F atoms in the relative rate studies would be reaction with O₃ to form FO, which, in the absence of a rapid reaction with O₃ (Atkinson et al., 2007) may undergo self reaction to reform F atoms, thus contributing to O₃ depletion but not to product formation. The identity (and fate) of the sulphur containing product remains unknown.

Title Page

Abstract

Introduction

Conclusions

References

Tables

Figures

◀

▶

◀

▶

Back

Close

Full Screen / Esc

Printer-friendly Version

Interactive Discussion

3.2 Kinetics of OH+SO₂F₂→ products (Reaction R2)

Figure 6 displays OH LIF profiles obtained following photolysis of H₂O₂ (Reaction R9) at 3 different [SO₂F₂]. The experiments were conducted using [H₂O₂]=5×10¹³ molecule cm⁻³ at *P*=300 Torr (N₂) and *T*=294 K. Note that large [SO₂F₂] of up to 2×10¹⁷ molecule cm⁻³ were used to significantly perturb the OH decay kinetics. Pseudo 1st-order conditions of [SO₂F₂] and [H₂O₂] \gg [OH] applied, therefore a simple expression was used to analyse the data. Since the OH was formed pseudo-instantaneously in the laser flash *C* approaches ∞ and expression (2) reduces to:

$$[\text{OH}]_t = A \times \exp(-Bt) \quad (6)$$

The insert in Fig. 6 shows the plot of the parameter of interest *B* (the pseudo first-order rate coefficient for OH decay) versus [SO₂F₂], to obtain *k*₂ (294 K)=(8.5±0.8)×10⁻¹⁶ cm³ molecule⁻¹ s⁻¹ from an un-weighted linear fit to the data. Note that the intercept value of around 100 s⁻¹ is consistent with slow loss of OH (in the absence of SO₂F₂ and associated impurities) due to reaction with the precursor H₂O₂ and diffusion/transport processes. It is entirely possible that the true value of *k*₂ is considerably smaller than this determination, as the sample of SO₂F₂ used in this work was of a quoted purity of 99%. If the (unknown) impurities of up to 1% react with OH with a rate coefficient of around 1×10⁻¹³ cm³ molecule⁻¹ s⁻¹ they could account for all of the OH reactivity observed in these experiments. Accordingly, based on the results of these experiments, we quote a conservative upper limit of *k*₂ (294 K)<1×10⁻¹⁵ cm³ molecule⁻¹ s⁻¹. We note that a considerable energetic barrier to product formation is anticipated, as strong S-F (~280 kJ mol⁻¹) or S=O (~520 kJ mol⁻¹) bonds must be broken if SO₂F₂ is to be destroyed in Reaction (R2). Reactions proceeding over such a barrier are characterised by an Arrhenius-type temperature dependence in *k*₂, which indicates that Reaction (R2) would proceed at a smaller rate at the much lower temperatures found throughout the troposphere above the boundary layer.

[Title Page](#)[Abstract](#)[Introduction](#)[Conclusions](#)[References](#)[Tables](#)[Figures](#)[◀](#)[▶](#)[◀](#)[▶](#)[Back](#)[Close](#)[Full Screen / Esc](#)[Printer-friendly Version](#)[Interactive Discussion](#)

3.3 Kinetics of $\text{O}_3 + \text{SO}_2\text{F}_2 \rightarrow \text{products}$ (Reaction R3)

In the course of the experimental study of Reaction (R1) it was noted that O_3 stored in blackened glass bulbs had a half-life of ≈ 14 days. To test whether the Reaction (R3) proceeds with an appreciable rate, a bulb was prepared in which an excess (5 Torr) of SO_2F_2 was added to a bulb containing 2 Torr of O_3 at a total pressure of 1000 Torr (synthetic air). The absorption cells and monochromator of the PLP-LIF apparatus were used to regularly monitor $[\text{O}_3]$ in samples taken from the mixture over the course of 3 weeks. No evidence for Reaction (R3) was observed, with O_3 loss proceeding at a similar rate to that observed in the absence of SO_2F_2 . An upper limit of k_3 (294 K) $< 1 \times 10^{-23} \text{ cm}^3 \text{ molecule}^{-1} \text{ s}^{-1}$ was estimated by assuming that all of the observed loss of O_3 was due to Reaction (R3).

3.4 The FTIR spectrum of SO_2F_2

The 0.5 cm^{-1} resolution, infra-red absorption spectrum of SO_2F_2 between ≈ 6 and $20 \mu\text{m}$ is displayed in Fig. 7. The major absorption bands at 1504.3, 1270.9, 887.0, 849.2, 551.9, 544.1 and 539.2 were observed to obey the Beer-Lambert expression for SO_2F_2 pressures up to ≈ 1 Torr (in a bath gas pressure of between 40 and 100 Torr). The accuracy of the absorption cross sections is expected to be determined largely by the measurement of the cell pressure and the mixing ratio in the storage bulb and should not be worse than $\pm 5\%$. At 0.5 cm^{-1} resolution, the strongest absorption features are at 1504.3 and 887 cm^{-1} , which have peak cross sections of 7.6 and $6.8 \times 10^{-18} \text{ cm}^2 \text{ molecule}^{-1}$, respectively and no rotational structure in the P and R envelopes is observed. At a resolution of 0.1 cm^{-1} , Q-branch splitting of the 1504.3 feature is more clearly observed and the peak cross section at this frequency increases to $\approx 1.1 \times 10^{-17} \text{ cm}^2 \text{ molecule}^{-1}$. The absorption features at 887.0 cm^{-1} (S-F stretch), 1270.4 cm^{-1} (S-O stretch) and 1504.3 cm^{-1} (S-O stretch) display rotational fine structure at the higher resolution. We note that the band positions and shapes are in good agreement with the spectrum reported in the "NIST Chemistry WebBook" (NIST Chem-

[Title Page](#)[Abstract](#)[Introduction](#)[Conclusions](#)[References](#)[Tables](#)[Figures](#)[◀](#)[▶](#)[◀](#)[▶](#)[Back](#)[Close](#)[Full Screen / Esc](#)[Printer-friendly Version](#)[Interactive Discussion](#)

istry WebBook, 2005). For the purpose of estimation of the integrated band strengths of SO₂F₂ the 0.5 cm⁻¹ resolution spectrum is used. Integrated band strengths (*S*) were calculated from:

$$S = \left(\frac{1}{p l} \right) \int_{\nu_1}^{\nu_2} \ln \left(\frac{I_0(\nu)}{I(\nu)} \right) d\nu \quad (7)$$

5 where *p* is the pressure of SO₂F₂ (atm), *l* is the optical pathlength (cm) and *I*₀(*ν*) and *I*(*ν*) are the intensities of transmitted radiation at wavenumber *ν* with and without SO₂F₂, respectively. The results are listed in Table 3. As a test of our method, the integrated band intensity of SF₆ was also determined using the same experimental set up to return a value of S(SF₆)=4750 cm⁻² atm⁻¹ for the 948 cm⁻¹ absorption band.
10 This value is in good agreement with a number of previous determinations (see Ko et al., 1993, for references). We are unaware of published integrated band strengths for SO₂F₂ with which to compare our data.

3.5 Uptake of SO₂F₂ onto aqueous surfaces (Reaction R4)

Despite the use of long contact times and variation of the pH between ≈2 and 12 no
15 loss of SO₂F₂ was observed, indicating a lack of irreversible loss processes and/or low solubility. The datapoints at individual contact times are summarised in Fig. 8, the solid fit lines being fits to the data of the form:

$$S_t = S_o \exp(-k_{\text{obs}} t) \quad (8)$$

where *t* is the contact time, *S*₀ and *S*_{*t*} are the signal of SO₂F₂ at time = zero and
20 *t*, respectively and *k*_{obs} is the pseudo first-order removal constant. The errors associated with each data point are of the order of 0.3% of the signal, and considerably smaller than the symbols in Fig. 8. The small errors, obtained by prolonged integration of the signal (≈100 s) at each contact time, were taken into account whilst performing weighted least squares fitting of the data. The values of *k*_{obs} obtained were:

15229

Title Page

Abstract

Introduction

Conclusions

References

Tables

Figures

◀

▶

◀

▶

Back

Close

Full Screen / Esc

Printer-friendly Version

Interactive Discussion

$(9.5 \pm 5) \times 10^{-4}$, $(10 \pm 4) \times 10^{-4}$ and $(5 \pm 4) \times 10^{-4}$ at pH values of 4.5, 12 and 2, respectively. These values of k_{obs} are close to the lower limit of first-order removal constants measurable with this apparatus, which is determined by signal noise. k_{obs} is related to the experimental uptake coefficient, γ_{expt} , via:

$$\gamma_{\text{expt}} = \frac{2 \cdot r \cdot k_{\text{obs}}}{\bar{c}} \quad (9)$$

where γ_{expt} is the experimentally derived, net ratio of collisions with the aqueous surface which remove SO_2F_2 from the gas phase, to the total number of collisions, r is the radius of the reactor (0.775 cm) and \bar{c} is the mean thermal velocity ($24\,060 \text{ cm s}^{-1}$ for SO_2F_2 at 277 K) derived from the Maxwell equation. From the fitted values of k_{obs} and Eq. (9), we derive upper limits to γ_{expt} of $6\text{--}9 \times 10^{-8}$ depending on pH. Consideration of possible systematic errors associated with calculation of the contact time (via flow rates and pressure measurements) leads us to present an upper limit of $\gamma_{\text{expt}} = 1 \times 10^{-7}$ for all experiments.

This result can be compared to the data of Cady and Misra (1974) who measured solubility and hydrolysis rates in alkaline solution. The rate coefficient for reaction of SO_2F_2 with OH^- was described by $k_{\text{OH}^-} = 1.67 \times 10^{12} \exp(-6593/T) \text{ L mol}^{-1} \text{ s}^{-1}$ which results in $k_{\text{OH}^-} = 77 \text{ L mol}^{-1} \text{ s}^{-1}$ at the temperature of our experiments. The solubility (H) of SO_2F_2 was given as $2.2 \times 10^{-2} \text{ mol L}^{-1} \text{ atm}^{-1}$ at 273 K. If the rate of removal of gas-phase SO_2F_2 is limited by reaction in solution these parameters can be related to the experimental uptake coefficient via:

$$\frac{1}{\gamma_{\text{expt}}} = \frac{1}{\alpha} + \frac{1}{\gamma_{\text{react}}} \quad (10)$$

with

$$\gamma_{\text{react}} = \frac{4HRT}{\bar{c}} \sqrt{D_l \cdot k_{\text{OH}^-} [\text{OH}]} \quad (11)$$

Title Page

Abstract

Introduction

Conclusions

References

Tables

Figures

◀

▶

◀

▶

Back

Close

Full Screen / Esc

Printer-friendly Version

Interactive Discussion

[Title Page](#)[Abstract](#)[Introduction](#)[Conclusions](#)[References](#)[Tables](#)[Figures](#)[◀](#)[▶](#)[◀](#)[▶](#)[Back](#)[Close](#)[Full Screen / Esc](#)[Printer-friendly Version](#)[Interactive Discussion](#)

α is the accommodation coefficient, D_l is the aqueous phase diffusion coefficient, which is close to $2 \times 10^{-5} \text{ cm}^2 \text{ s}^{-1}$ for neutral, closed shell species in aqueous solutions at ambient temperatures (Seinfeld, 1986). Taking the literature values of H and k_{OH^-} (Cady and Misra, 1974) and the concentration ($1 \times 10^{-2} \text{ M}$) of OH^- from our experiment at $\text{pH}=12$ gives $\gamma_{\text{react}} \approx 2 \times 10^{-7}$. As the contribution to γ_{expt} from the accommodation coefficient α (which is probably between 1×10^{-3} and 1) will be small, $\gamma_{\text{react}} \approx \gamma_{\text{expt}}$. The calculated value of γ is thus in acceptable agreement with the measured upper limit to γ_{react} from the WWFT experiments. Cady and Misra (1974) found significantly lower loss rates of SO_2F_2 in acidified solutions (pH as low as 2), suggesting that only loss to alkaline aqueous surfaces is of significance.

3.6 Atmospheric implications

In the following section we make some simple calculations on the lifetime of SO_2F_2 with respect to various loss processes in different parts of the atmosphere and, based on this, a qualitative estimate of its global warming potential.

3.6.1 Reaction with OH in the troposphere

We have shown that SO_2F_2 reacts only very slowly with the OH radical. A lower limit to its tropospheric lifetime with respect to loss by reaction with OH can be obtained by combining a diurnally and globally averaged OH concentration of $1 \times 10^6 \text{ molecule cm}^{-3}$ with the rate coefficient of $k_2 \leq 1 \times 10^{-15} \text{ cm}^3 \text{ molecule}^{-1} \text{ s}^{-1}$ as presented here. The resultant lifetime exceeds 30 years and is strictly a lower limit for a number of reasons. Firstly, as already mentioned our determination of the rate coefficient k_2 is an upper limit, as loss of OH was (probably) driven by reactive impurities in our SO_2F_2 sample. Secondly, the absence of any easily abstractable atoms in SO_2F_2 implies a significant barrier to reaction and that the rate coefficient will most likely decrease rapidly with altitude in the troposphere as the temperature decreases. Thus the true lifetime of SO_2F_2 with respect to reaction by OH could easily be an order of magnitude longer

than the lower limit calculated here.

3.6.2 Heterogeneous loss/dry deposition of SO₂F₂ in the boundary layer

The value of γ_{expt} obtained in this study can be used to estimate the lifetime of atmospheric SO₂F₂ with respect to its uptake to aqueous surfaces. For uptake coefficients lower than $\approx 10^{-3}$, the following expression defines the lifetime (τ , s) in the presence of aerosol of loading A (cm² cm⁻³):

$$\tau = \frac{4}{\gamma_{\text{expt}} \cdot \bar{c} \cdot A} \quad (12)$$

Following Sander and Crutzen (1996) we assume an average surface area density of $A=5 \times 10^{-7}$ cm²/cm³ for the marine boundary layer, which results in a lower limit to the SO₂F₂ lifetime of 100 years in this environment. This must however be considered a lower limit to the lifetime with respect to aerosol loss, as atmospheric aerosol is nearly always acidic and, as shown by Cady and Misra (1974) SO₂F₂ does not interact strongly with aqueous neutral or acidic surfaces. Indeed, using expression (11) (and using the coefficients for solubility and hydrolysis of Cady and Misra) and we can calculate a value of $\gamma_{\text{react}} \approx 2 \times 10^{-9}$, which would be representative of uptake to the ocean surface with an average temperature of 20°C and pH of ≈ 8 ($[\text{OH}]^- = 1 \times 10^{-6}$ mol L⁻¹). Note that at pH values greater than 7.5, hydrolysis is dominated by reaction with OH⁻ and direct reaction with water can be neglected. The value of $\gamma=2 \times 10^{-9}$ can be used to calculate the deposition velocity to the ocean using:

$$v_{\text{dep}} = \frac{\gamma \cdot \bar{c}}{4} \quad (13)$$

which gives us $v_{\text{dep}}=1.2 \times 10^{-5}$ cm s⁻¹. Combining the deposition velocity with recent measurements of the SO₂F₂ concentration of ≈ 1 ppt (Möhle, 2006) and the ocean surface area of $\approx 3.6 \times 10^8$ km² allows us to calculate that $\approx 6 \times 10^3$ kg of SO₂F₂ will

Title Page

Abstract

Introduction

Conclusions

References

Tables

Figures

◀

▶

◀

▶

Back

Close

Full Screen / Esc

Printer-friendly Version

Interactive Discussion

annually be lost to the oceans. This number is negligibly small in comparison to the present annual atmospheric release rate, which is clearly larger than 10^6 kg/year.

3.6.3 Loss of SO_2F_2 in the stratosphere

We have shown that SO_2F_2 does react efficiently with $\text{O}(^1\text{D})$ atoms, thus opening a potential sink in the stratosphere. A rough guide to its lifetime with respect to reaction with $\text{O}(^1\text{D})$ can be obtained by comparison to N_2O , which has a stratospheric lifetime of about 130 years, mainly (90%) a result of photolysis, the remainder due to reaction with $\text{O}(^1\text{D})$. The lifetime of N_2O with respect to reaction with $\text{O}(^1\text{D})$ can thus be estimated as >1000 years. As the rate coefficient (k_{1b}) for reaction of $\text{O}(^1\text{D})$ with SO_2F_2 is \approx a factor two slower than N_2O with $\text{O}(^1\text{D})$ we can estimate a lifetime in excess of 2000 years with respect to loss by Reaction (R1). Although the VUV spectrum of SO_2F_2 was not studied in this work, we can also coarsely evaluate the lifetime of SO_2F_2 with respect to photolysis in the stratosphere by comparison with N_2O . Within the important wavelength region for N_2O photolysis (185–210 nm), the absorption cross sections of SO_2F_2 (Pradayrol et al., 1996) are consistently a factor of five to ten less than those of N_2O , which would convert to a photolytic lifetime in excess of 500 years. Accurate study of the SO_2F_2 cross sections in the relevant wavelength range, and calculation of the J-value with an appropriate radiation transfer model would be useful to confirm this. Clearly however, SO_2F_2 is too long lived in the lower stratosphere to contribute significantly to the sulphate layer.

3.6.4 SO_2F_2 as a greenhouse gas?

In the absence of an important chemical sink process for SO_2F_2 once released into the atmosphere, we must consider its potential role as an atmospheric greenhouse gas. The SO_2F_2 IR absorption features in the $814\text{--}918\text{ cm}^{-1}$ spectral range are located within the “atmospheric window” and, via model calculations of the atmospheric sources, sinks and distribution of SO_2F_2 , the integrated band intensity (Table 3) can be

Title Page

Abstract

Introduction

Conclusions

References

Tables

Figures

◀

▶

◀

▶

Back

Close

Full Screen / Esc

Printer-friendly Version

Interactive Discussion

used to estimate the greenhouse warming potential (GWP) of this gas. Whilst an in-depth study is beyond the scope of this publication, and would require a more complete set of SO_2F_2 IR spectral measurements, we can compare the integrated band intensity with that of another, long lived fluorinated sulphur species, SF_6 , which has one of the largest GWPs (over a 100 year period) of all known atmospheric trace gases. The integrated band intensity for the SF_6 absorption feature at $\approx 950\text{ cm}^{-1}$ is circa 5000 (see Sect. 3.4) a factor of just 3.3 larger than SO_2F_2 . We note that the absorption feature of SO_2F_2 at $\approx 7.9\ \mu\text{m}$ also absorbs (albeit more weakly) within the atmospheric window. Given the long lifetime of SO_2F_2 and the expected increase in its production rate over the next decades it is plausible that this species could indeed become an important greenhouse gas. This needs to be thoroughly evaluated in detailed modelling studies.

4 Conclusions

In a series of laboratory studies we have investigated a number of reactions that could contribute to the chemical removal of SO_2F_2 from the atmosphere. Experimental data was obtained for reaction of SO_2F_2 with excited oxygen atoms ($\text{O}(^1\text{D})$), the OH radical, O_3 and with aqueous surfaces. The reaction with $\text{O}(^1\text{D})$ proceeds both by energy transfer (quenching of $\text{O}(^1\text{D})$, $\approx 55\%$) and product formation ($\approx 45\%$), with an overall rate coefficient of k_1 (220–300 K) $= (1.3 \pm 0.2) \times 10^{-10}\text{ cm}^3\text{ molecule}^{-1}\text{ s}^{-1}$. Upper limits for the rate coefficients ($\text{cm}^3\text{ molecule}^{-1}\text{ s}^{-1}$) for reaction of SO_2F_2 with OH ($k_2 < 1 \times 10^{-15}$) and O_3 ($k_3 < 1 \times 10^{-23}$) were obtained. No evidence for loss to aqueous surfaces was obtained. The kinetic data allowed us to estimate very long chemical lifetimes for SO_2F_2 in all parts of the lower atmosphere, which, together with our measurements of infrared absorption bands in the atmospheric window, suggest that SO_2F_2 may have a large greenhouse warming potential.

[Title Page](#)[Abstract](#)[Introduction](#)[Conclusions](#)[References](#)[Tables](#)[Figures](#)[◀](#)[▶](#)[◀](#)[▶](#)[Back](#)[Close](#)[Full Screen / Esc](#)[Printer-friendly Version](#)[Interactive Discussion](#)

Acknowledgements. T. J. Dillon acknowledges the support of the Max Planck Society in the provision of a research grant. We are indebted to P. Crutzen for providing motivation and for helpful discussions.

ACPD

7, 15213–15249, 2007

**Atmospheric
chemistry of SO₂F₂**

T. J. Dillon et al.

Title Page

Abstract

Introduction

Conclusions

References

Tables

Figures

◀

▶

◀

▶

Back

Close

Full Screen / Esc

Printer-friendly Version

Interactive Discussion

EGU

References

- Atkinson, R., Baulch, D. L., Cox, R. A., Crowley, J. N., Hampson, R. F., Hynes, R. G., Jenkin, M. E., Kerr, J. A., Rossi, M. J., and Troe, J.: IUPAC Subcommittee for gas kinetic data evaluation, evaluated kinetic data: <http://www.iupac-kinetic.ch.cam.ac.uk/>, 2007.
- 5 Blitz, M. A., Dillon, T. J., Heard, D. E., Pilling, M. J., and Trought, I. D.: Laser induced fluorescence studies of the reactions of O(¹D₂) with N₂, O₂, N₂O, CH₄, H₂, CO₂, Ar, Kr and n-C₄H₁₀, Phys. Chem. Chem. Phys., 6, 2162–2171, 2004.
- Cady, G. H. and Misra, S.: Hydrolysis of sulfuryl fluoride, Inorg. Chem., 13, 837–841, 1974.
- Carl, S. A.: A highly sensitive method for time-resolved detection of O(¹D) applied to precise determination of absolute O(¹D) reaction rate constants and O(³P) yields, Phys. Chem. Chem. Phys., 7, 4051–4053, 2005.
- 10 Crutzen, P. J.: The possible importance of CSO for the sulfate layer of the stratosphere, Geophys. Res. Lett., 3, 73–76, 1976.
- Dillon, T. J., Horowitz, A., and Crowley, J. N.: Absolute rate coefficients for the reactions of O(¹D) with a series of n-alkanes, Chem. Phys. Lett., 14, 12–16, 2007.
- 15 Dillon, T. J., Karunanandan, R., and Crowley, J. N.: The reaction of IO with CH₃SCH₃: products and temperature dependent rate coefficients by laser induced fluorescence, Phys. Chem. Chem. Phys., 8, 847–855, 2006.
- Dunlea, E. J. and Ravishankara, A. R.: Kinetic studies of the reactions of O(¹D) with several atmospheric molecules, Phys. Chem. Chem. Phys., 6, 2152–2161, 2004a.
- 20 Dunlea, E. J. and Ravishankara, A. R.: Measurement of the rate coefficient for the reaction of O(¹D) with H₂O and re-evaluation of the atmospheric OH production rate, Phys. Chem. Chem. Phys., 6, 3333–3340, 2004b.
- Dunlea, E. J., Ravishankara, A. R., Strekowski, R. S., Nicovich, J. M., and Wine, P. H.: Temperature-dependent quantum yields for O(³P) and O(¹D) production from photolysis of O₃ at 248 nm, Phys. Chem. Chem. Phys., 6, 5484–5489, 2004.
- European Union: Competent Authority Report, Document III-B7, 2005.
- Fickert, S., Adams, J. W., and Crowley, J. N.: Activation of Br₂ and BrCl via uptake of HOBr onto aqueous salt solutions, J. Geophys. Res., 104, 23 719–23 727, 1999.
- 30 Fickert, S., Helleis, F., Adams, J. W., Moortgat, G. K., and Crowley, J. N.: Reactive uptake of ClNO₂ on aqueous bromide solutions, J. Phys. Chem., 102, 10 689–10 696, 1998.
- Karunanandan, R., Hölscher, D., Dillon, T. J., Horowitz, A., and Crowley, J.: Reaction of HO

Title Page

Abstract

Introduction

Conclusions

References

Tables

Figures

◀

▶

◀

▶

Back

Close

Full Screen / Esc

Printer-friendly Version

Interactive Discussion

- with glycolaldehyde, HOCH₂CHO: Rate coefficients (240–362 K) and mechanism, *J. Phys. Chem. A*, 111, 897–908, 2007.
- Ko, M. K. W., Sze, N. D., Wang, W. C., Shia, G., Goldman, A., Murcray, F. J., Murcray, D. G., and Rinsland, C. P.: Atmospheric Sulfur-Hexafluoride – Sources, Sinks and Greenhouse Warming, *J. Geophys. Res.*, 98, 10 499–10 507, 1993.
- Kollman, W. S.: Sulfuryl fluoride (Vikane) Risk Characterisation Document Volume III. Environmental Fate, Environmental Monitoring Branch, Department of Pesticide Regulation, California Environmental Protection Agency, Sacramento, CA, 2006.
- Mühle, J., Harth, C. M., Salameh, P. K., Miller, B. R., Porter, L. W., Fraser, P. J., Greally, B. R., O'Doherty, S., and Weiss, R. F.: Global Measurements of Atmospheric Sulfuryl Fluoride (SO₂F₂), in *Eos. Trans. AGU*, 87(52), Fall Meet. Suppl., Abstract A53B-0191, 2006.
- NIST Chemistry WebBook: NIST Standard Reference Database Number 69, <http://webbook.nist.gov/chemistry/>, edited by: Linstrom, P. J. and Mallard, W. G., 2005.
- Pradayrol, C., Casanovas, A. M., Deharo, I., Guelfucci, J. P., and Casanovas, J.: Absorption coefficients of SF₆, SF₄, SOF₂ and SO₂F₂ in the vacuum ultraviolet, *J. Phys. III*, 6, 603–612, 1996.
- Raber, W. H. and Moortgat, G. K.: Photooxidation of selected carbonyl compounds in air, in: *Problems and Progress in Atmospheric Chemistry*, edited by: Barker, J. R., World Scientific Publishing Co. Pte. Ltd, Singapore, 2000.
- Sander, R. and Crutzen, P. J.: Model study indicating halogen activation and ozone destruction in polluted air masses transported to the sea, *J. Geophys. Res.*, 101, 9121–9138, 1996.
- Sander, S. P., Friedl, R. R., Golden, D. M., Kurylo, M. J., Huie, R. E., Orkin, V. L., Moortgat, G. K., Ravishankara, A. R., Kolb, C. E., Molina, M. J., and Finlayson-Pitts, B. J.: Chemical kinetics and photochemical data for use in atmospheric studies: Evaluation Number 15, Jet Propulsion Laboratory, National Aeronautics and Space Administration/Jet Propulsion Laboratory/California Institute of Technology, Pasadena, CA, 2006.
- Schofield, K.: Rate constants for gaseous interactions of O(¹D₂) and O(¹S₀) – Critical evaluation, *J. Photochem.*, 9, 55–68, 1978.
- Seinfeld, J. H.: *Atmospheric chemistry and physics of air pollution*, John Wiley and Sons, 1986.
- Strekowski, R. S., Nicovich, J. M., and Wine, P. H.: Temperature-dependent kinetics study of the reactions of O(¹D₂) with N₂ and O₂, *Phys. Chem. Chem. Phys.*, 6, 2145–2151, 2004.
- Takahashi, K., Takeuchi, Y., and Matsumi, Y.: Rate constants of the O(¹D) reactions with N₂, O₂, N₂O, and H₂O at 295 K, *Chem. Phys. Lett.*, 410, 196–200, 2005.

**Atmospheric
chemistry of SO₂F₂**

T. J. Dillon et al.

Title Page

Abstract

Introduction

Conclusions

References

Tables

Figures

◀

▶

◀

▶

Back

Close

Full Screen / Esc

Printer-friendly Version

Interactive Discussion

Teruel, M. A., Dillon, T. J., Horowitz, A., and Crowley, J. N.: Reaction of O(³P) with the alkyl iodides: CF₃I, CH₃I, CH₂I₂, C₂H₅I, 1-C₃H₇I and 2-C₃H₇I, Phys. Chem. Chem. Phys., 6, 2172–2178, 2004.

5 Wollenhaupt, M., Carl, S. A., Horowitz, A., and Crowley, J. N.: Rate coefficients for reaction of OH with acetone between 202 and 395 K, J. Phys. Chem. A, 104, 2695–2705, 2000.

ACPD

7, 15213–15249, 2007

**Atmospheric
chemistry of SO₂F₂**

T. J. Dillon et al.

Title Page

Abstract

Introduction

Conclusions

References

Tables

Figures

◀

▶

◀

▶

Back

Close

Full Screen / Esc

Printer-friendly Version

Interactive Discussion

EGU

Table 1. Determination of rate coefficients for the reactions $O(^1D)+X\rightarrow$ products.

X	T/K	H-donor	range of [X] ^a	$k(T)$ ^b
SO ₂ F ₂	300	<i>n</i> -C ₆ H ₁₄	0–20.9	1.29±0.20
SO ₂ F ₂	300	<i>n</i> -C ₆ H ₁₄	0–20.9	1.25±0.20
SO ₂ F ₂	300	<i>n</i> -C ₆ H ₁₄	0–34.0	1.22±0.06
SO ₂ F ₂	298	<i>n</i> -C ₆ H ₁₄	0–25.5	1.39±0.12
SO ₂ F ₂	297	<i>n</i> -C ₅ H ₁₂	0–19.4	1.20±0.20
SO ₂ F ₂	222	<i>n</i> -C ₅ H ₁₂	0–27.0	1.47±0.08
SO ₂ F ₂	218	<i>n</i> -C ₆ H ₁₄	2.4–40.5	1.39±0.10
<i>n</i> -C ₅ H ₁₂	297	<i>n</i> -C ₅ H ₁₂	0–9.3	5.4±0.4
<i>n</i> -C ₆ H ₁₄	300	<i>n</i> -C ₆ H ₁₄	0–10.4	5.8±0.5
N ₂	300	<i>n</i> -C ₆ H ₁₄	0–172.0	0.35±0.02
N ₂	297	<i>n</i> -C ₆ H ₁₄	0–212.0	0.33±0.02
N ₂	297	none ^c	0–277.0	0.30±0.04
N ₂	297	H ₂ O	0–106.0	0.38±0.05
N ₂	297	<i>n</i> -C ₆ H ₁₄	0–212.0	0.30±0.02
H ₂ O	297	H ₂ O	0–17.8	1.94±0.13
N ₂ O	296	<i>n</i> -C ₅ H ₁₂	0–37.1	1.45±0.08
N ₂ O	296	<i>n</i> -C ₅ H ₁₂	0–49.5	1.49±0.08

Notes:

^a units of concentration = 10^{13} molecule cm⁻³;

^b units for $k(T)$ = 10^{-10} cm³ molecule⁻¹ s⁻¹;

^c no H-atom donor was added to the reaction mixture, however OH was observed from reactions of O(¹D) with impurities (e.g. H₂O, H₂) in the bath gas.

Atmospheric chemistry of SO₂F₂

T. J. Dillon et al.

Title Page

Abstract

Introduction

Conclusions

References

Tables

Figures

◀

▶

◀

▶

Back

Close

Full Screen / Esc

Printer-friendly Version

Interactive Discussion

Table 2. Determination of the O(³P) product yield (k_{1a}/k_1) in Reaction (R1).

T/K	[SO ₂ F ₂] ^a	[N ₂] ^a	correction ^b	k_{1a}/k_1
296	7.6	30.8	15%	0.52±0.01
296	13.8	56.0	10%	0.57±0.01
296	4.6	19.0	20%	0.57±0.01
296	11.0	44.0	11%	0.55±0.01
296	6.0	25.0	16%	0.55±0.01
225	9.1	37.0	15%	0.58±0.01
225	16.3	53.0	10%	0.54±0.01
225	16.5	66.0	8%	0.55±0.02
225	13.2	45.0	12%	0.54±0.01

Notes:

^a in units of 10¹³ molecule cm⁻³.^b Correction for “background” O(³P) according to Eq. (4), see text for details.[Title Page](#)[Abstract](#)[Introduction](#)[Conclusions](#)[References](#)[Tables](#)[Figures](#)[I◀](#)[▶I](#)[◀](#)[▶](#)[Back](#)[Close](#)[Full Screen / Esc](#)[Printer-friendly Version](#)[Interactive Discussion](#)

Atmospheric chemistry of SO₂F₂

T. J. Dillon et al.

Table 3. Integrated band strengths for SO₂F₂.

ν (cm ⁻¹)	1504.3	1270.9	849.2, 887.0	551.9, 544.1, 539.2
λ (μ m)	6.648	7.868	11.78, 11.27	18.12, 18.38, 18.55
Range (cm ⁻¹)	1455–1540	1220–1310	810–920	500–595
S (cm ⁻¹ [cm atm] ⁻¹)	984	616	1394	343

Title Page

Abstract

Introduction

Conclusions

References

Tables

Figures

I◀

▶I

◀

▶

Back

Close

Full Screen / Esc

Printer-friendly Version

Interactive Discussion

Atmospheric
chemistry of SO_2F_2

T. J. Dillon et al.

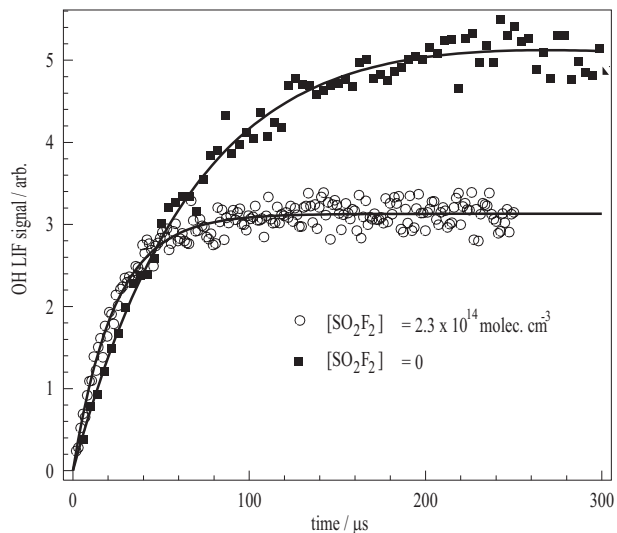


Fig. 1. OH LIF profiles recorded at two different $[\text{SO}_2\text{F}_2]$ in determination of k_1 (300 K). Experimental conditions were $P=42$ Torr, $T=300$ K, $[\text{O}_3]=1 \times 10^{12}$ and $[\text{n-C}_6\text{H}_{14}]=2.1 \times 10^{13} \text{ molecule cm}^{-3}$. The solid lines are fits using expression (2) to obtain the kinetic parameter C .

[Title Page](#)[Abstract](#)[Introduction](#)[Conclusions](#)[References](#)[Tables](#)[Figures](#)[◀](#)[▶](#)[◀](#)[▶](#)[Back](#)[Close](#)[Full Screen / Esc](#)[Printer-friendly Version](#)[Interactive Discussion](#)

EGU

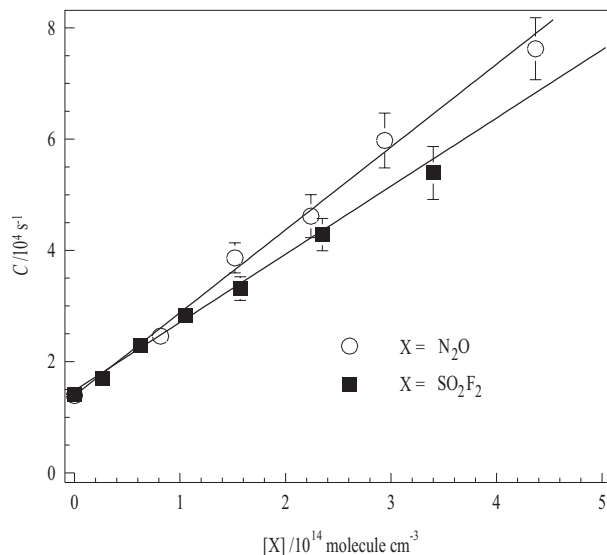


Fig. 2. Bimolecular plot of C vs. $[\text{SO}_2\text{F}_2]$ used to determine k_1 (300 K) $= (1.23 \pm 0.06) \times 10^{-10} \text{ cm}^3 \text{ molecule}^{-1} \text{ s}^{-1}$. The intercept value of $\sim 14\,000 \text{ s}^{-1}$ is consistent with the use of $[\text{n-C}_6\text{H}_{14}] = 2 \times 10^{13} \text{ molecule cm}^{-3}$ to convert $\text{O}(^1\text{D})$ to OH (Reaction R7). The plot also shows the results of an experiment to determine k_{11} (296 K) $= (1.45 \pm 0.08) \times 10^{-10} \text{ cm}^3 \text{ molecule}^{-1} \text{ s}^{-1}$.

[Title Page](#)
[Abstract](#)
[Introduction](#)
[Conclusions](#)
[References](#)
[Tables](#)
[Figures](#)
[◀](#)
[▶](#)
[◀](#)
[▶](#)
[Back](#)
[Close](#)
[Full Screen / Esc](#)
[Printer-friendly Version](#)
[Interactive Discussion](#)

Atmospheric chemistry of SO_2F_2

T. J. Dillon et al.

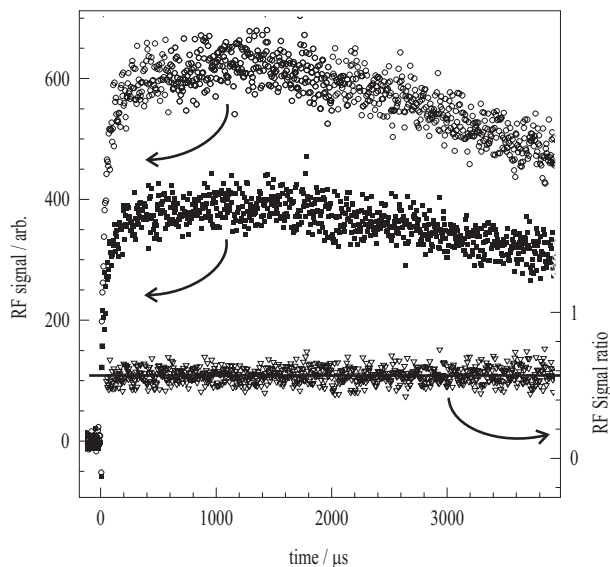


Fig. 3. $\text{O}(^3\text{P})$ generated in $\text{O}(^1\text{D}) + \text{SO}_2\text{F}_2 \rightarrow \text{products}$ (Reaction R1) with $[\text{SO}_2\text{F}_2] = 1.4 \times 10^{14} \text{ molecule cm}^{-3}$ (middle trace). Also displayed is the $\text{O}(^3\text{P})$ RF signal obtained in a back-to-back experiment in which $\text{O}(^1\text{D})$ reacts (Reaction R10) with a kinetically similar $[\text{N}_2] = 5.6 \times 10^{14} \text{ molecule cm}^{-3}$ (upper trace). As the yield of $\text{O}(^3\text{P})$ in Reaction (R10) is known to be unity, the yield of $\text{O}(^3\text{P})$ in Reaction (R1) $= k_{1a}/k_1 = (0.56 \pm 0.01)$ was calculated from the ratio of RF signal intensities (lower trace) plotted on the right axis.

Title Page

Abstract

Introduction

Conclusions

References

Tables

Figures

◀

▶

◀

▶

Back

Close

Full Screen / Esc

Printer-friendly Version

Interactive Discussion

EGU

Atmospheric
chemistry of SO_2F_2

T. J. Dillon et al.

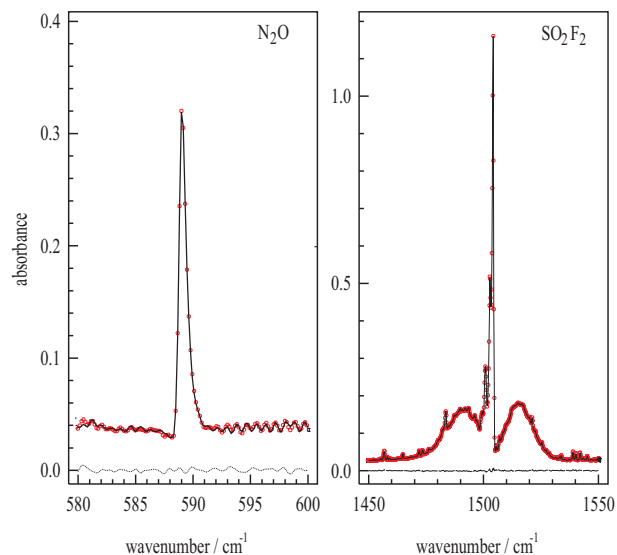


Fig. 4. Raw FTIR spectral data for SO_2F_2 and N_2O in relative rate studies. The data points (circles) were determined after photolysis, the solid lines are scaled reference spectra (obtained before photolysis) with the scaling factor (depletion factor) obtained by least squares fitting. The broken lines are the fit residuals.

[Title Page](#)[Abstract](#)[Introduction](#)[Conclusions](#)[References](#)[Tables](#)[Figures](#)[◀](#)[▶](#)[◀](#)[▶](#)[Back](#)[Close](#)[Full Screen / Esc](#)[Printer-friendly Version](#)[Interactive Discussion](#)

EGU

Atmospheric
chemistry of SO_2F_2

T. J. Dillon et al.

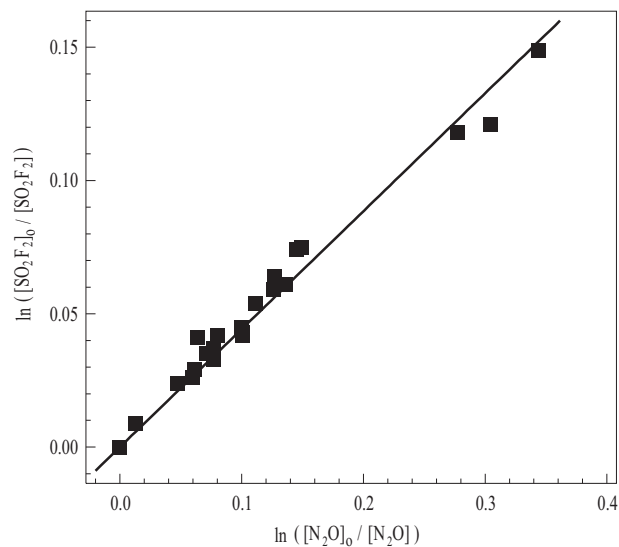


Fig. 5. Relative rate plot of depletion of N_2O (reference compound) versus depletion of SO_2F_2 to determine the ratio $k_{1b}/k_{11}=(0.44\pm 0.01)$ from a linear fit to the data with the intercept forced through zero.

[Title Page](#)[Abstract](#)[Introduction](#)[Conclusions](#)[References](#)[Tables](#)[Figures](#)[◀](#)[▶](#)[◀](#)[▶](#)[Back](#)[Close](#)[Full Screen / Esc](#)[Printer-friendly Version](#)[Interactive Discussion](#)

EGU

Atmospheric chemistry of SO₂F₂

T. J. Dillon et al.

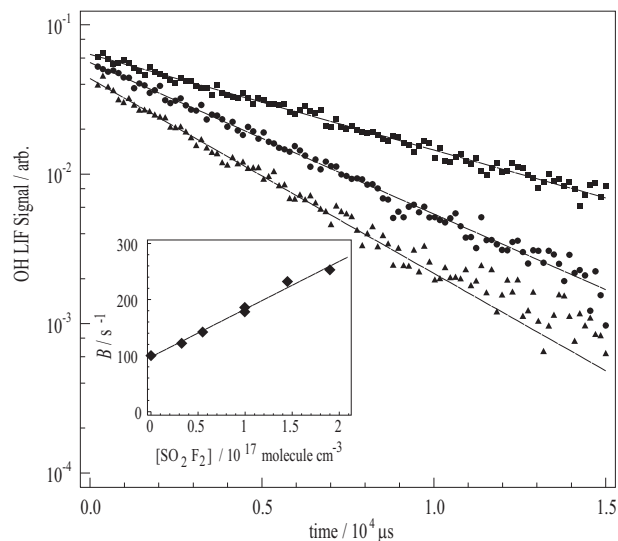


Fig. 6. Determination of k_2 ($T=294$ K) for reaction of $\text{OH}+\text{SO}_2\text{F}_2\rightarrow\text{products}$. The three OH LIF profiles show data collected at: $[\text{SO}_2\text{F}_2]/\text{molecule cm}^{-3}=0$ (upper trace), 9.96×10^{16} (middle trace) and 19.0×10^{16} (lower trace). The straight lines depict fits with expression (6) to obtain values of parameter B . The insert show the plot of B versus $[\text{SO}_2\text{F}_2]$ to yield k_2 (294 K) $= (8.5\pm 0.8)\times 10^{-16} \text{ cm}^3 \text{ molecule}^{-1} \text{ s}^{-1}$.

Title Page

Abstract

Introduction

Conclusions

References

Tables

Figures

◀

▶

◀

▶

Back

Close

Full Screen / Esc

Printer-friendly Version

Interactive Discussion

EGU

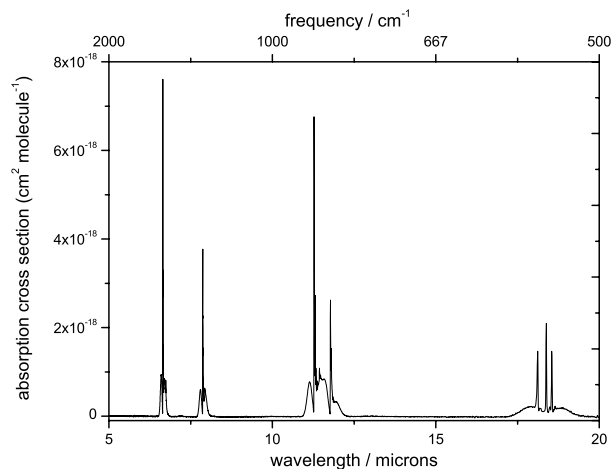


Fig. 7. The FTIR spectrum of SO_2F_2 at 0.5 cm^{-1} resolution. The strong absorption feature around 1500 cm^{-1} was used in the relative rate study. Integrated band intensities are listed in Table 3.

[Title Page](#)[Abstract](#)[Introduction](#)[Conclusions](#)[References](#)[Tables](#)[Figures](#)[I◀](#)[▶I](#)[◀](#)[▶](#)[Back](#)[Close](#)[Full Screen / Esc](#)[Printer-friendly Version](#)[Interactive Discussion](#)

EGU

Atmospheric
chemistry of SO_2F_2

T. J. Dillon et al.

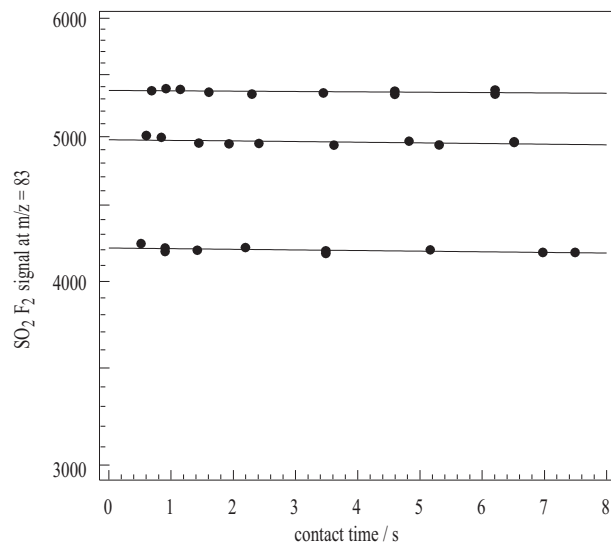


Fig. 8. The uptake of SO_2F_2 onto aqueous surfaces of different pH (2, 12 and 4.5 for the upper, middle and lowest trace, respectively). Different concentrations of SO_2F_2 and/or mass spectrometer sensitivity is the cause of the vertical displacement of the data from each experiment.

[Title Page](#)[Abstract](#)[Introduction](#)[Conclusions](#)[References](#)[Tables](#)[Figures](#)[I◀](#)[▶I](#)[◀](#)[▶](#)[Back](#)[Close](#)[Full Screen / Esc](#)[Printer-friendly Version](#)[Interactive Discussion](#)

EGU